

Introduction II: Opacities and dust radiative transfer

Ciska Kemper

3 July 2023

Francisca Kemper, ICREA Research Professor
ICE-CSIC / ICREA / IEEC
ciska@ice.csic.es

1 Extinction

Consider light passing through a medium filled with absorbing particles:

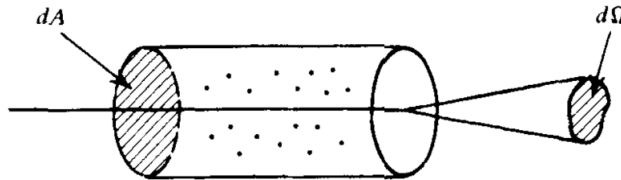


Figure 1: Ray passing through a medium of absorbers. The column has length L and the absorbing grains have radius a . The volume number density of absorbing particles is n_d . Figure adopted from Rybicki & Lightman (1979).

The reduction of starlight over a length dL is:

$$\frac{dI}{I} = -n_d C_{\text{ext}} dL \quad (1)$$

with C_{ext} being the extinction cross-section, which can also be written as the extinction efficiency applied to the geometrical cross-section:

$$C_{\text{ext}} = Q_{\text{ext}} \cdot \pi a^2 \quad (2)$$

Integrating over the full path-length L gives:

$$I = I_0 e^{-\tau} \quad (3)$$

with

$$\tau = \int n_d dL \cdot C_{\text{ext}} = N_d C_{\text{ext}} \quad (4)$$

N_d is the column density of dust, or the total number of grains in the column towards the star.

The (wavelength-dependent) reduction in magnitude A_λ can be expressed as:

$$\begin{aligned} A_\lambda &= -2.5 \log \left(\frac{I}{I_0} \right) = -2.5 \log e^{-\tau} \\ &\approx 1.086 \tau = 1.086 N_d C_{\text{ext}} = 1.086 N_d \pi a^2 Q_{\text{ext}} \end{aligned} \quad (5)$$

The interstellar extinction curve shows the wavelength dependence of the reduction in magnitude, with respect to the reduction in V-band magnitude A_V .

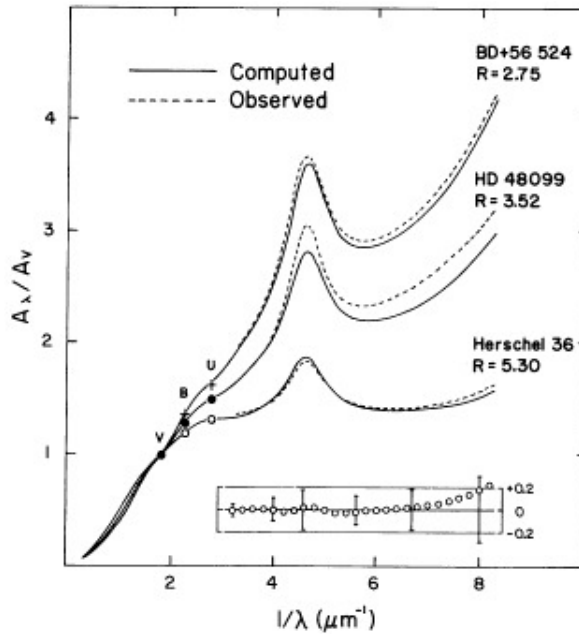


Figure 2: Interstellar extinction curve, measured towards three different background stars. Figure taken from Cardelli et al. (1989).

Sometimes the extinction curve is also shown in terms of color excess. The color excess is defined as $E_{\lambda_1-\lambda_2} = A_{\lambda_1} - A_{\lambda_2}$, and is usually expressed with respect to the B-V color: E_{B-V} .

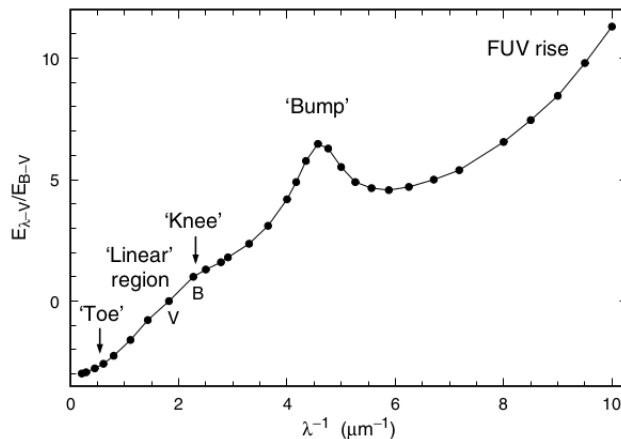


Figure 3: Interstellar extinction curve with respect to the B-V color, with several spectral features indicated. Figure taken from Whittet (2003).

The intercept with the vertical axis can be calculated by having $\lambda \rightarrow \infty$, and this is known as the reddening law:

$$\lim_{\lambda \rightarrow \infty} \frac{E_{\lambda-V}}{E_{B-V}} = \frac{A_V}{E_{B-V}} = R_V \quad (6)$$

In the Milky Way, $R_V \approx 3.1$, but this is just an average, and values may vary between 2.7 and 4.5, especially in other galaxies. Fig. 4 shows the comparison between the Milky Way, and the Large and Small Magellanic Clouds, to illustrate this.

For a distribution of grain sizes, $n(a) da$ represents the number of grains per unit volume in the size range from a to $a + da$. Thus, we can write for the extinction caused by grains of a range of sizes:

$$A_\lambda = 1.086\pi L \int a^2 Q_{\text{ext}}(a) n(a) da \quad (7)$$

2 Opacities

Following Whittet (2003), the extinction efficiencies of materials can be separated out in two components for absorption and scattering:

$$Q_{\text{ext}} = Q_{\text{abs}} + Q_{\text{sca}} \quad (8)$$

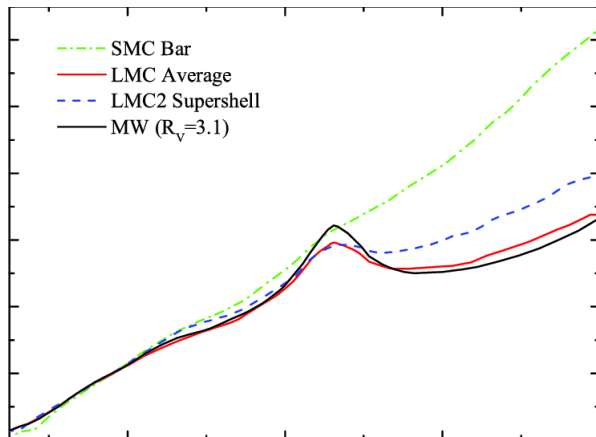


Figure 4: Comparison between the interstellar extinction curves measured for the Milky Way (averaged over multiple sightlines), the Small Magellanic Cloud, and the Large Magellanic Cloud. In the case of the Large Magellanic Clouds, sightlines within the massive star formation region 30 Doradus have been considered separately from the rest of the galaxy. Figure after e.g. Gordon et al. (2003).

These efficiencies are functions of two quantities, a dimensionless size parameter,

$$X = \frac{2\pi a}{\lambda} \quad (9)$$

and a composition parameter, the complex refractive index of the grain material:

$$m = n - ik \quad (10)$$

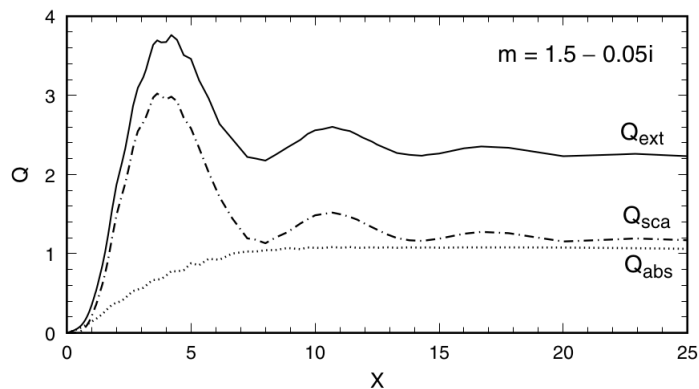


Figure 5: Results of Mie theory calculations for spherical grains of refractive index $m = 1.5 - 0.05i$, plotted against size parameter X . Figure taken from Whittet (2003).

In principle, n and k are wavelength dependent, and can be used to calculate wavelength-dependent Q_{abs} and Q_{ext} , given a grain size and grain shape. For pure dielectric materials $k = 0$, and $m = n \approx c_1 + c_2\lambda^{-2}$. Thus m is in principle wavelength-dependent, but only weakly, as c_2 is usually small. Real materials, such as silicates and ices, are not purely dielectric, and k has a small, non-zero value. For strong absorbers, such as metals, $k \approx n$, or both vary strongly with wavelength.

When $X \ll 1$ the interaction between the grain and light is in the *Rayleigh domain*. In this case, following Whittet (2003), the small particle approximation can be derived (see Bohren & Huffman, 1983, Chapter 5):

$$Q_{\text{sca}} \approx \frac{8}{3} \left(\frac{2\pi a}{\lambda} \right)^4 \left| \frac{m^2 - 1}{m^2 + 2} \right|^2 \quad (11)$$

and

$$Q_{\text{abs}} \approx \frac{8\pi a}{\lambda} \text{Im} \left\{ \frac{m^2 - 1}{m^2 + 2} \right\} \quad (12)$$

Again, for pure dielectrics, m is real and by approximation constant with wavelength as stated above. In that case Q_{abs} becomes 0, and $Q_{\text{sca}} \propto \lambda^{-4}$, a situation called Rayleigh scattering. In general, $(m^2 - 1)/(m^2 + 2)$ is only weakly dependent on wavelength for materials that are not strongly absorbing, and then $Q_{\text{sca}} \propto \lambda^{-4}$ and $Q_{\text{abs}} \propto \lambda^{-1}$.

In the case of a strong wavelength dependence, e.g. spectral features, the situation becomes more complicated, and a more sophisticated approach is needed to determine $Q_{\text{sca}}(\lambda)$ and $Q_{\text{abs}}(\lambda)$. Fig. 6 shows an example of wavelength-dependent n , k values.

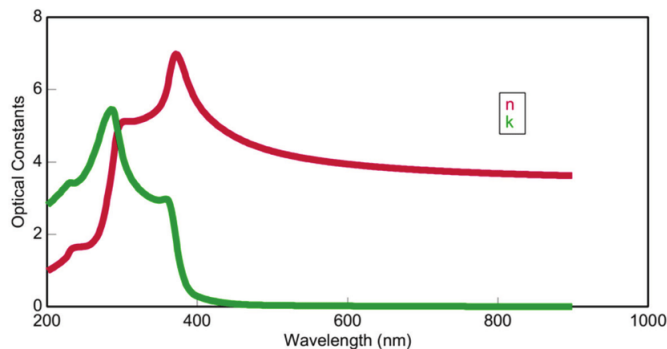


Figure 6: Example of n , k as a function of wavelength, here presented for crystalline silicon.

For spherical grains, Mie theory can be applied (Mie, 1908; van de Hulst, 1957) to determine $Q_{\text{abs}}(\lambda)$ and $Q_{\text{ext}}(\lambda)$ from n and k , while for non-spherical grains more complex treatments are required, see e.g. Bohren & Huffman (1983). Useful approximations to calculate $Q_{\text{abs}}(\lambda)$ and $Q_{\text{ext}}(\lambda)$ of non-spherical grain sizes are found in the continuous distribution of ellipsoids (CDE; Bohren & Huffman, 1983), arbitrarily-shaped particles (e.g. Min et al., 2006), or hollow spheres (Min et al., 2005). It is shown that all three of these show similar results in Q_{abs} and Q_{ext} , while the hollow spheres and CDE offer relative ease of calculation.

3 Radiative transfer

Radiative transfer equation $I(\nu)$ is controlled by radiative transfer.

Define $\kappa(\nu)$ as the absorption coefficient per unit length of path s .

Absorption only (foreground screen): the change in intensity as light travels through the ISM:

$$dI(\nu)/ds = -\kappa(\nu)I(\nu) \quad (13)$$

Define optical depth τ_ν as $d\tau_\nu = \kappa(\nu)ds$ or

$$\tau_\nu = \int \kappa(\nu)ds \quad (14)$$

Optical depth can be seen as the probability that a photon will interact with a particle while passing through a medium.

$\tau < 1$: optically thin

$\tau > 1$: optically thick

Thus:

$$\kappa_\nu = \frac{d\tau_\nu}{ds} \quad (15)$$

$$\frac{dI(\nu)}{ds} = -I(\nu)\frac{d\tau_\nu}{ds} \quad (16)$$

$$-\frac{1}{I(\nu)}dI(\nu) = d\tau_\nu \quad (17)$$

$$-\ln I(\nu) = \tau_\nu + C \quad (18)$$

$$I(\nu) = I_{\nu 0}e^{-\tau_\nu} \quad (19)$$

Full radiative transfer equation So far, we have looked at absorption only. However, a medium may also be emitting radiation.

Thus, radiative transfer becomes:

$$\frac{dI(\nu)}{ds} = -\kappa(\nu)I(\nu) + j(\nu) \quad (20)$$

Emission: $j(\nu)$, defined so that $j(\nu)dVd\nu d\Omega dt$ is the energy emitted by volume element dV , in frequency width $d\nu$, during time interval dt , into solid angle $d\Omega$.

Using $d\tau_\nu = \kappa(\nu)ds$:

$$\frac{dI(\nu)}{d\tau_\nu} = -I(\nu) + S(\nu) \quad (21)$$

with the source function $S(\nu) = \frac{j(\nu)}{\kappa(\nu)}$

- Formal solution:

multiply by e^{τ_ν} :

$$e^{\tau_\nu} \frac{dI(\nu)}{d\tau_\nu} = -I(\nu)e^{\tau_\nu} + S(\nu)e^{\tau_\nu} \quad (22)$$

$$\frac{dI(\nu)e^{\tau_\nu}}{d\tau_\nu} - I(\nu)e^{\tau_\nu} = -I(\nu)e^{\tau_\nu} + S(\nu)e^{\tau_\nu} \quad (23)$$

$$\frac{dI(\nu)e^{\tau_\nu}}{d\tau_\nu} = S(\nu)e^{\tau_\nu} \quad (24)$$

$$(25)$$

define $\mathcal{I} = I(\nu)e^{\tau_\nu}$ and $\mathcal{S} = S(\nu)e^{\tau_\nu}$

thus:

$$\frac{d\mathcal{I}}{d\tau_\nu} = \mathcal{S} \quad (26)$$

with solution:

$$\mathcal{I}(\tau_\nu) = \mathcal{I}(0) + \int_0^{\tau_\nu} \mathcal{S}(\tau'_\nu) d\tau'_\nu \quad (27)$$

rewrite with $I(\nu)$, $S(\nu)$ again:

$$I(\nu)e^{\tau_\nu} = I_{\nu 0}e^0 + \int_0^{\tau_\nu} S(\nu)e^{\tau'_\nu} d\tau'_\nu \quad (28)$$

$$I(\nu) = I_{\nu 0}e^{-\tau_\nu} + \int_0^{\tau_\nu} S(\nu)e^{-(\tau_\nu - \tau'_\nu)} d\tau'_\nu \quad (29)$$

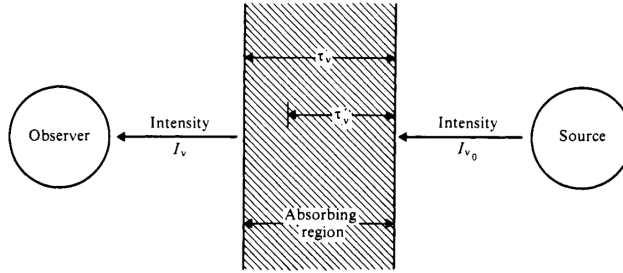


Figure 7: Schematic drawing defining intensities after absorption. Figure from Dyson & Williams (1997).

Interpretation:

Resulting intensity = initial intensity diminished by absorption + integrated source function diminished by remaining absorption.

4 Thermal dust emission

Blackbody radiation Blackbody radiation: a blackbody is a perfect absorber at all wavelengths/frequencies, and a perfect emitter.

Emitted intensity depends solely on T , ν , and therefore Kirchhoff's Law applies:

$$j(\nu) = \kappa(\nu)B_\nu(T) \quad (30)$$

with the *Planck Function* $B_\nu(T)$:

$$B_\nu(T) = \frac{2h\nu^3}{c^2} \frac{1}{e^{h\nu/kT} - 1} \quad (31)$$

We speak of *thermal radiation* when $S(\nu) = B_\nu(T)$ (Kirchhoff's law) and of *blackbody radiation* when $I(\nu) = B_\nu(T)$

Thermal radiation becomes blackbody radiation when the emitting medium is optically thick:

Assume:

$$S(\nu) = B_\nu(T) \tag{32}$$

So:

$$\lim_{\tau_\nu \rightarrow \infty} I(\nu) = I_{\nu_0} e^{-\tau_\nu} + S(\nu)(1 - e^{-\tau_\nu}) \tag{33}$$

$$I(\nu) = B_\nu(T) \tag{34}$$

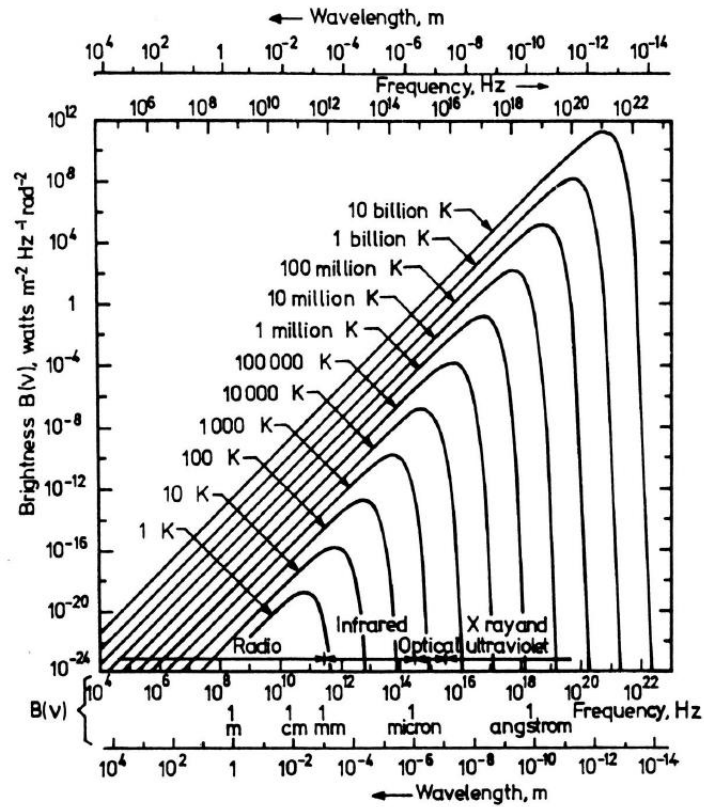


Figure 8: Spectrum of blackbody radiation at different temperatures. This is Fig. 1.11 from Rybicki & Lightman (1979), reproduced from Kraus (1966).

Properties of the Planck Function: We can derive the following properties:

- $h\nu \ll kT$: low energy, large wavelength, Rayleigh-Jeans approximation:

$$e^{h\nu/kT} - 1 = \frac{h\nu}{kT} + \dots \quad (35)$$

$$\Rightarrow I_\nu^{\text{RJ}}(T) = \frac{2\nu^2}{c^2} kT \quad (36)$$

- $h\nu \gg kT$: high energy, short wavelength, Wien approximation:

$$\frac{1}{e^{h\nu/kT} - 1} \approx \frac{1}{e^{h\nu/kT}} \quad (37)$$

$$\Rightarrow I_\nu^{\text{W}}(T) = \frac{2h\nu^3}{c^2} e^{-h\nu/kT} \quad (38)$$

- Monotonicity with T . Two blackbody curves with different do not intersect, the one with higher T lies entirely above the other.
- Wien Displacement Law: ν_{max} at the peak of $B_\nu(T)$ satisfies

$$\frac{\partial B_\nu}{\partial \nu} = 0 \quad (39)$$

$$\Rightarrow \frac{\nu_{\text{max}}}{T} = 5.88 \times 10^{10} \text{ Hz K}^{-1} \quad (40)$$

Characteristic temperatures: The following can be derived:

- *Brightness temperature* T_b satisfies: $I(\nu) = B_\nu(T_b)$. In radio-astronomy where Rayleigh-Jeans is applicable: $I(\nu) = \frac{2\nu^2}{c^2} kT_b$ or $T_b = \frac{c}{2\nu^2 k} I(\nu)$. Basically: try to fit emitter with a blackbody. Insert $T_b \propto I(\nu)$ and $T \propto B_\nu(T)$ into:

$$I(\nu) = I_{\nu 0} e^{-\tau_\nu} + B_\nu(T)(1 - e^{-\tau_\nu}) \quad (41)$$

$$T_b = T_{b0} e^{-\tau_\nu} + T(1 - e^{-\tau_\nu}) \quad (42)$$

For large τ_ν : $T_b \rightarrow T$

- *Colour temperature* T_c
 - Shape approaches blackbody form, but does not have the appropriate absolute value
 - Fit blackbody shape to data using $I(\nu) = C \cdot B_\nu(T_c)$
 - Often done by only measuring peak position and applying Wien Displacement Law

Modified blackbodies:

$$\int F(\lambda)Q_{\text{abs}}(a, \lambda) d\lambda = \int Q_{\text{abs}}(a, \lambda)B(\lambda, T_g) d\lambda \quad (43)$$

$$B(\lambda, T_g) = \frac{2hc^2}{\lambda^5} \frac{1}{e^{hc/k\lambda T_g} - 1} \quad (44)$$

References

- Bohren, C. F., & Huffman, D. R. 1983, Absorption and scattering of light by small particles (New York: Wiley)
- Cardelli, J. A., Clayton, G. C., & Mathis, J. S. 1989, ApJ, 345, 245, doi: 10.1086/167900
- Dyson, J. E., & Williams, D. A. 1997, The physics of the interstellar medium, 2nd edn., The Graduate Series in Astronomy (Bristol: Institute of Physics Publishing)
- Gordon, K. D., Clayton, G. C., Misselt, K. A., Landolt, A. U., & Wolff, M. J. 2003, ApJ, 594, 279, doi: 10.1086/376774
- Kraus, J. D. 1966, Radio astronomy (McGraw-Hill Book Company)
- Mie, G. 1908, Annalen der Physik, 330, 377, doi: 10.1002/andp.19083300302
- Min, M., Hovenier, J. W., & de Koter, A. 2005, A&A, 432, 909, doi: 10.1051/0004-6361:20041920
- Min, M., Hovenier, J. W., Dominik, C., de Koter, A., & Yurkin, M. A. 2006, J. Quant. Spectrosc. Radiative Transfer, 97, 161, doi: 10.1016/j.jqsrt.2005.05.059

- Rybicki, G. B., & Lightman, A. P. 1979, *Radiative Processes in Astrophysics* (New York: John Wiley & Sons)
- van de Hulst, H. C. 1957, *Light Scattering by Small Particles* (New York: John Wiley & Sons)
- Whittet, D. C. B. 2003, *Dust in the galactic environment*, 2nd edn. (London: Institute of Physics Publishing)